Measurement of Signal-to-Noise Ratio and Parallel Imaging

4

Scott B. Reeder

CONTENTS

4.1 **Introduction** *49*

4.2 **SNR Measurement in MR Images** *49*

4.3 **SNR and Parallel Imaging** *50*

4.4 **Alternative Methods to Measure SNR** *52*
4.4.1 Multiple Acquisition Method *52*
4.4.2 Difference Method *55*
4.4.3 SNR Ratio Method *57*
4.4.4 Direct Calculation of the g-Factor *57*

4.5 **Special Considerations** *58*
4.5.1 TSENSE *57*
4.5.2 Self-Calibrating Parallel-Acceleration Methods *58*
4.5.3 Measurement of SNR with Multi-Phase Contrast-Enhanced Imaging *59*

4.6 **Summary and Conclusion** **59**

References *61*

4.1 Introduction

The signal-to-noise ratio (SNR) of an image is a fundamental quantitative measure of MR image quality and system performance, and has enormous impact on the diagnostic quality of clinical studies. The SNR measurements provide a direct means for comparison of signal levels between different imaging method, patients, reconstruction methods, coils, and even different scanner systems. It is one of the essential measures of system performance and is used routinely in quality assurance protocols that monitor scanner performance (Price et al. 1990).

S. B. Reeder, MD, PhD
Departments of Radiology and Medical Physics, E3/311 CSC, University of Wisconsin, 600 Highland Avenue, Madison, WI 53792-3252, USA

The advent of parallel imaging with the development of SMASH (Sodickson and Manning 1997) and SENSE (Pruessmann et al. 1999), as well as other parallel imaging methods (Griswold et al. 2000, 2002; McKenzie et al. 2002; Kellman et al. 2001; cf. Chap. 2), has had tremendous impact on modern clinical scanning protocols. Parallel acceleration methods are commonly used to reduce acquisition time, with the trade-off that SNR of the resulting images will be reduced. For this reason, the ability to make accurate SNR measurements to measure the performance of parallel imaging applications is even more essential.

Unfortunately, routine methods commonly used to measure SNR with single coil imaging applications are no longer valid when using parallel imaging methods. Noise becomes distributed unevenly across the image (as discussed in Chap. 3) and application of routine measurement methods can lead to highly erroneous SNR measurements. Great caution must be used when measuring SNR with parallel-imaging applications.

In this chapter we review correct methods for the measurement of SNR in conventional single coil images, and review the underlying assumptions that are made. The concept of local noise amplification, characterized by the geometry, or "g-factor" is then discussed, and reasons why the application of conventional methods for SNR measurement will fail when applied to images acquired with parallel imaging. Finally, three methods for SNR measurement that are compatible with parallel-imaging applications are discussed.

4.2 SNR Measurement in MR Images

The signal-to-noise ratio, is exactly what the name implies, the signal in an image at a specific location, divided by the noise at that same location. "Signal" is commonly measured as the *average* signal in a small region of interest. "Noise" is typically quantified as the

root mean square (RMS) amplitude of the white noise that is superimposed on the signal. For MR systems, it has been shown that the noise has a Gaussian distribution with zero mean (McVeigh et al. 1985). Conveniently, the RMS amplitude of a Gaussian distribution equals its standard deviation, such that SNR of a *complex* image is measured as the ratio of the average signal (S) to the standard deviation of the noise (σ), i.e.,

$$\mathrm{SNR} = \frac{S}{\sigma} \tag{1}$$

After Fourier transformation into the spatial domain, noise is *evenly distributed* throughout the image. For this reason, SNR can be measured for single-coil acquisitions as the quotient of the average signal in a region of interest (ROI) within the object, and the standard deviation of the noise in a ROI outside the object, free from signal or artefact (i.e., "air"), as diagrammed in Fig. 4.1.

Most clinical MR images are presented as magnitude images, rather than complex images, and this greatly alters the behavior of the background noise, as shown in Fig. 4.2. After the magnitude operation, the noise distribution is skewed and no longer has a zero mean. In addition, the apparent standard deviation of the noise is *lower* than the true standard deviation, by a factor of 0.655, as described by Henkelman 1985).

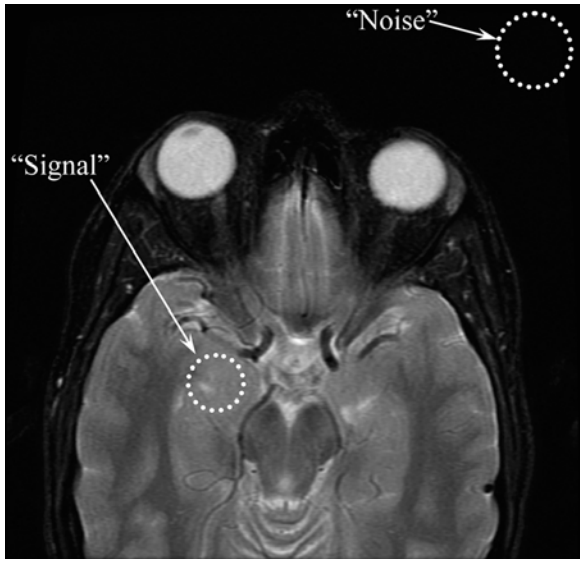

Fig. 4.1. Measurement of signal-to-noise ratio (SNR) from an image acquired with a single receive coil and *no* parallel imaging acceleration is determined from the ratio of the average signal in the "Signal" ROI and the standard deviation of the noise in the "Noise" ROI, placed outside the object. This approach assumes that noise is uniform across the image. In addition, a correction factor for the underestimation of noise must be made.

The noise in the magnitude image follows the statistics of a Rayleigh distribution (Edelstein et al. 1984), and measuring the standard deviation of the background noise from a magnitude image will overestimate SNR by approximately 53% (=1/0.655). In addition, as can be seen by the profile shown in Fig. 4.3, taking the magnitude of a complex image changes neither the signal nor the noise in object if the SNR is sufficiently high (≥5), even though the noise in the background region has been significantly altered, as was shown in Fig. 4.2; therefore, measurement of SNR from magnitude images acquired with single-coil acquisitions can be determined from the ratio of the average signal (S) in a "signal" ROI, and the apparent standard deviation (σ_{app}) within a "noise" ROI outside the object, and the appropriate correction factor, i.e.,

$$\mathrm{SNR}_{\mathrm{MAG}} = 0.655\frac{S}{\sigma_{\mathrm{app}}} \tag{2}$$

For multi-coil applications without parallel accelerations, images can be recombined in several different ways, although the "square root of sum of squares" method proposed by Roemer (et al. 1990) is a commonly used approach. Measurement of SNR from multi-coil images reconstructed using this approach can made in a similar manner as single coil acquisitions, except the correction factor changes slightly. For four or more coils, the correction factor is approximately 0.70 (Constantinides et al. 1997).

4.3 SNR and Parallel Imaging

The use of parallel imaging will degrade the SNR performance of the reconstructed image through two mechanisms (see also Chap. 3). First, SNR is reduced as a result of decreased data sampling, i.e.,

$$\mathrm{SNR}_R = \frac{\mathrm{SNR}_0}{\sqrt{R}}, \tag{3}$$

where R (≥1) is the "reduction" or acceleration factor used in the acquisition, and SNR_0 is the signal-to-noise ratio of the equivalent unaccelerated image.

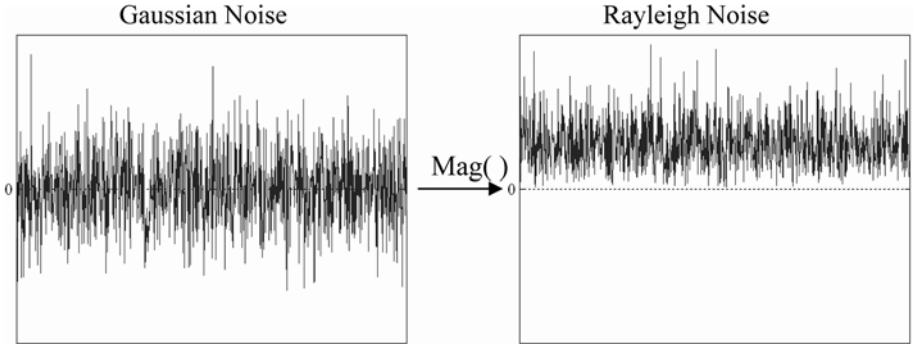

Fig. 4.2. The noise in a complex MR image has a Gaussian distribution with a zero mean and standard deviation,σ. With magnitude images, however, the noise has a Rayleigh distribution, with non-zero mean and an apparent standard deviation σ_{app}=0.655σ, an *under-estimation* of the true noise level.

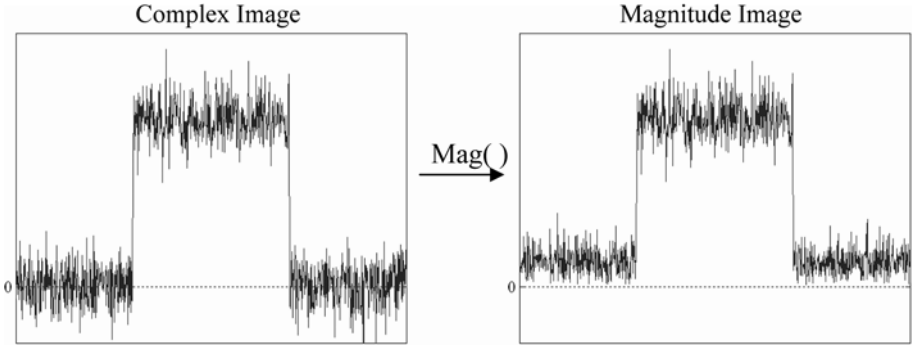

Fig. 4.3. The noise in a complex MR image has a Gaussian distribution with a zero mean and standard deviation, σ. With magnitude images, however, the noise in the background has a reduced apparent noise level, whereas noise in the region of signal remains unaffected if the SNR is sufficiently high.

This equation simply reflects that the image will be noisier when less data is acquired, directly analogous to signal averaging. This equation holds for low acceleration factors (R=2–3) with well designed coils, and the SNR performance of parallel imaging is simply related to the square root of the total scan time.

There is a second cause of SNR degradation that commonly occurs with parallel imaging. This degradation is a result of noise amplification that occurs with parallel imaging and reflects the ability of the parallel reconstruction algorithm to unwrap superimposed (aliased) pixels given a certain coil geometry (Pruessmann et al. 1999). This additional SNR degradation can be quantified with the so-called geometry or "g" factor (cf. Chap. 3), such that

$$\mathrm{SNR}_R = \frac{\mathrm{SNR}_0}{g\sqrt{R}}. \qquad (4)$$

Equation (4) can be rearranged as

$$g = \frac{\mathrm{SNR}_0}{\mathrm{SNR}_R\sqrt{R}}, \qquad (5)$$

which is the mathematical definition of the g-factor.

The g-factor always has a value of one or more and may be non-uniform across the image. It reflects an increase in local noise, not a decrease in signal, which is unchanged between the accelerated and unaccelerated images. It is also important to realize that the g-factor is highly dependent on the coil geometry and the resulting sensitivity profiles, the orientation of the phase-encoding direction, the acceleration factor (R), and the field of view (FOV). In addition, the object itself may have indirect but significant impact on the g-factor by the effective image masking on the sensi-

tivity profiles, due to the shape and size of the object. Typically, the g-factor is greatest in locations farthest from the coil elements, often near the center of the FOV in areas of critical clinical importance. Equation (5) can be further simplified by recalling that the signal from the accelerated and unaccelerated images, S_0 and S_R, respectively, are equal,

$$g = \frac{S_0/\sigma_0}{S_R/\sigma_R\sqrt{R}} = \frac{\sigma_R}{\sigma_0\sqrt{R}}, \quad (6)$$

demonstrating that only the noise from the accelerated and unaccelerated images must be measured in order to determine the g-factor.

4.4 Alternative Methods to Measure SNR

As characterized by the g-factor, noise is not evenly distributed in accelerated images reconstructed with parallel-imaging methods. Attempts to measure SNR using the approach described above may be incorrect if the noise level in the "noise" ROI is lower than in the area of interest where the signal is measured. For example, Fig. 4.4 shows a noisy one-dimensional magnitude image for the case where noise is uniformly distributed and a case where there is a higher level of noise at the center of the image. The true SNR at this location is very poor. Although measurement of the average signal at this location is unaffected, estimation of noise in an area outside the object (background noise) would be greatly underestimated, and *SNR would be erroneously overestimated.*

Figure 4.5 shows phantom images acquired with increasing acceleration factors. Although the average signal remains unchanged throughout the images, geographic regions of increased noise are very apparent, particularly at higher acceleration factors

Similar increases in noise can also be seen with clinical images, even with modest acceleration factors. Figure 4.6 shows an example of "in and out of phase" T1-weighted spoiled-gradient imaging in a patient with alcoholic steatohepatitis, acquired with an acceleration of two. Subtle increased noise at the center of the images is caused by local noise amplification that occurs with parallel imaging from a g-factor that is greater than one.

So how do we measure SNR in an accelerated image where the g-factor must be considered? A successful method for the measurement of SNR from images acquired with parallel-imaging accelerations must account for non-uniform noise throughout the image. In this chapter, three SNR measurement methods that account for non-uniform noise across the image are discussed. These methods include a "multiple acquisition" method, a "difference" method, and direct calculation of the g-factor using measured coil sensitivities.

4.4.1 Multiple Acquisition Method

A robust, although time-consuming method for measuring SNR, known as the "multiple acquisition" method, is performed by repeating an image acquisition many times. This method can be performed with magnitude images. Assuming that the scanner is stable and the signal does not vary from image to

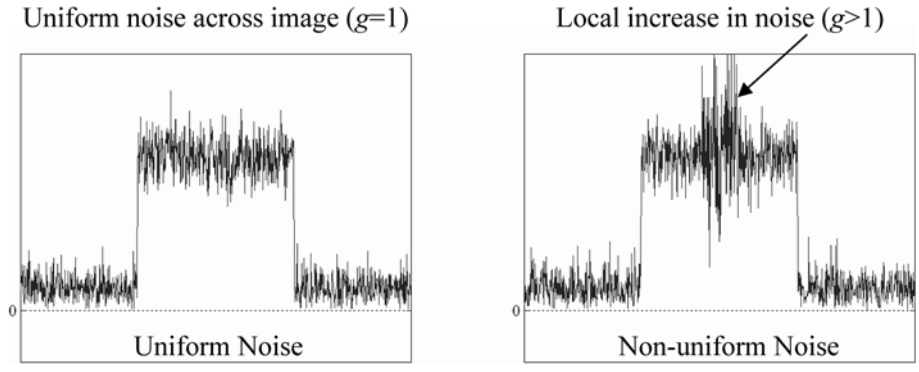

Fig. 4.4. Profile of image with noise with uniform noise across the image (left) compared to the profile of an image with non-uniform noise centrally (right). Even though the average signal is unchanged at this location, the noise is clearly higher at this location than elsewhere in the image. Accurate measurements of local SNR must take this local variation in noise into account.

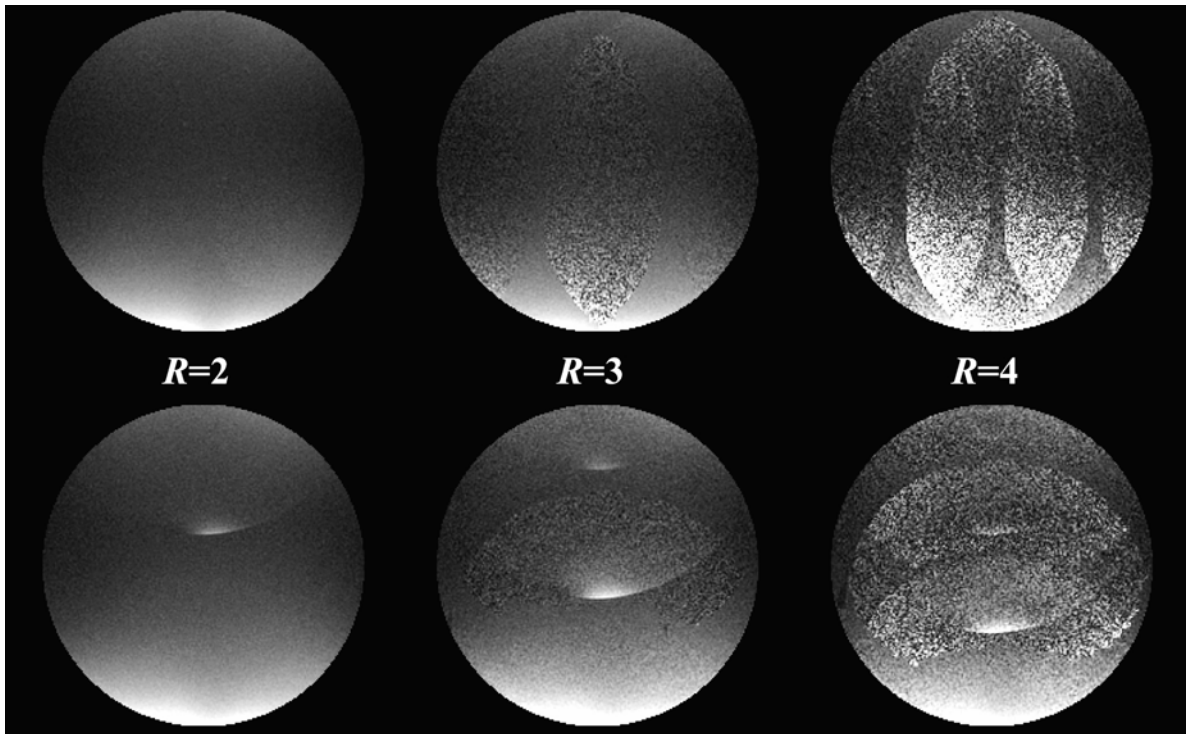

Fig. 4.5. Subjective increase in local noise of spoiled gradient-echo phantom images that worsens with increasing acceleration. Phase-encoding direction is left–right (*top row*) and up–down (*bottom row*), and the window/level is the same for all images. Although the average signal is similar between the images, there are areas of locally increased noise which severely degrade portions of the image, especially at higher acceleration factors.

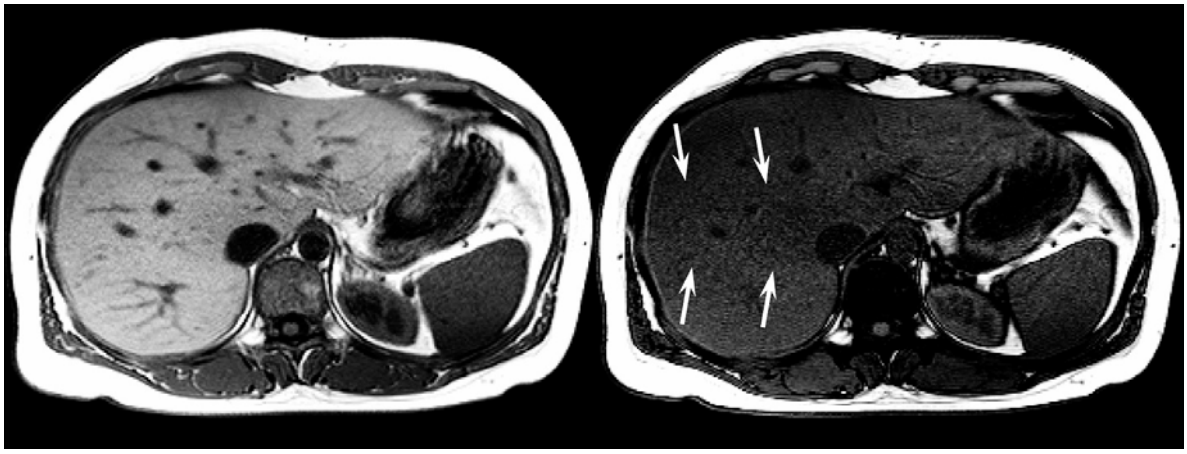

Fig. 4.6. In-phase (*left*) and out-of-phase (*right*) spoiled gradient-echo images of the liver in patient with alcoholic steatohepatitis. The drop in signal in the out-of-phase image reveals subtle increased local noise in the center of the liver (*arrows*), resulting from noise amplification characterized by $g>1$. The increase in noise near the center of the image is not caused by lower coil sensitivity, which would cause a decrease in signal, not an increase in noise.

image, the SNR can be determined on a *pixel-by-pixel basis*, providing a high-resolution "SNR image." The SNR at each pixel, determined using the multiple acquisition method is given by

$$\mathrm{SNR} = \frac{S_t}{\sigma_t}, \tag{7}$$

where S_t is the average signal and σ_t is the standard deviation of the signal measured from multiple images acquired over time for each pixel. This allows the measurement of SNR on a pixel-by-pixel basis, and permits accurate measurement of local SNR despite the presence of spatial variation in image noise. This method is shown schematically in Fig. 4.7 for a series of images with non-uniform noise throughout the image, demonstrating how SNR is measured for each pixel across the image.

With the multiple acquisition method, typically 30–300 images are acquired. The number of images will determine the uncertainty on the measurement of SNR itself. The more images that are acquired, the less uncertainty there is in the SNR measurement. Through standard propagation of error methods (Bevington and Robinson 1992), it can easily be shown that for an N image acquisition, the error on the SNR measurement itself is

$$\sigma_{\mathrm{SNR}} = \mathrm{SNR}\sqrt{\frac{2}{N}}. \tag{8}$$

For example, if the approximate SNR of an image was 20, and one desired an error of less than ±2 (i.e., 10%), one would need to acquire 200 or more images. An error of less than ±4 (i.e., 20%) would require 50 or more images.

It is important to discuss two important assumptions of the multiple acquisition approach. Firstly, it is imperative that there be no inherent signal fluctuations over time. Any signal fluctuations would be interpreted as noise and incorrectly decrease the apparent SNR measurement. The second major assumption is that the noise follows Gaussian statistics even when using magnitude images. As was shown and described in Fig. 4.3, the noise in a background region changes from Gaussian to Rayleigh statistics after the magnitude operation, causing an apparent (and erroneous) decrease in the standard deviation of the noise; however, the noise in an area of relatively high signal is unaffected and will maintain Gaussian statistics. Estimates of noise in this region are unaffected by the magnitude operation. In general, this assumption is true so long as SNR is approximately 5 or higher (Henkelman 1985). Above this SNR, noise is unaffected by the magnitude operation and SNR measurements made using the multiple acquisition method are valid. This also implies that SNR measurements made in background regions or areas of very low SNR are inherently incorrect. Masking of SNR values below 5 or a similar value can be performed to avoid display of these areas.

Finally, the multiple acquisition method can be extended to direct measurement of g-factor images. Two sets of images are required, one acquired without acceleration and the other with some acceleration factor, R. From Eqs. (5) or (6), a g-factor "image" can be easily calculated. Regions of SNR <5 can be

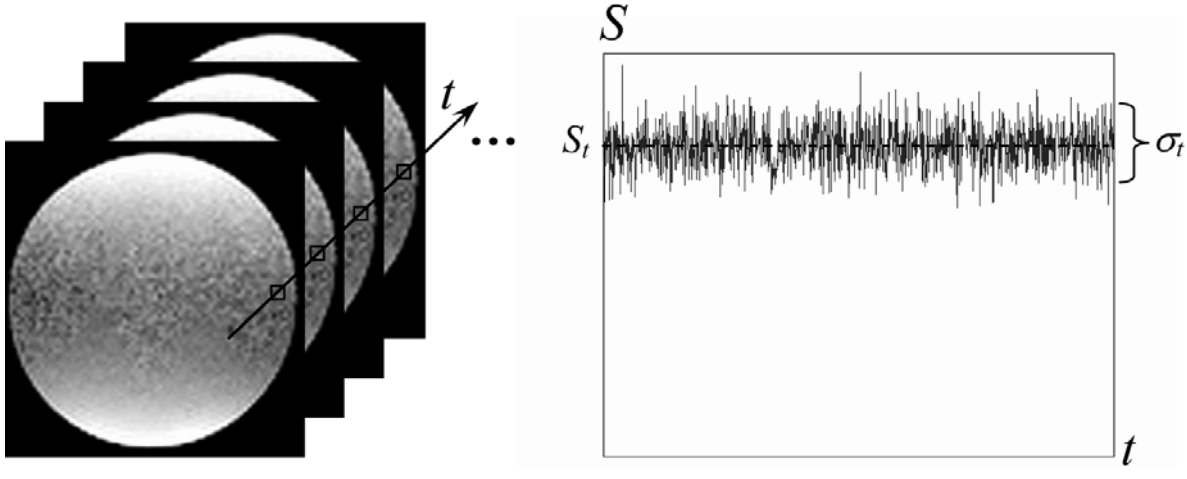

Fig. 4.7. The multiple acquisition method. Multiple identical images are acquired. For each pixel, the signal and standard deviation are measured over time, permitting direct calculation of the SNR for that pixel.

masked to zero. Examples of calculated g-factor images are shown in Fig. 4.8. From these images, it can be seen that the g-factor is highly dependent on position within the image, the acceleration factor, and the orientation of the phase-encoding direction.

Although the multiple acquisition approach is robust and accurate, it can be time-consuming and, in general, may be impractical for in vivo SNR measurements. It is best reserved for phantom experiments or specific in vivo cases where motion and physiological variations do not create signal fluctuations that would incorrectly be interpreted as noise.

4.4.2 Difference Method

A second method for measuring SNR can be performed through the acquisition of only two images, instead of large numbers (Price et al. 1990; Firbank et al. 1999). In this approach, an estimate of the mean signal is obtained from a small ROI from the sum of the images, and the standard deviation of the difference of the images is obtained from the same ROI. Because the noise is estimated from the difference of two magnitude images in a region with relatively high signal, the noise will maintain Gaussian statistics. The local SNR within the ROI from two images, $\mathbf{S}_1$ and $\mathbf{S}_2$, is then calculated as (Reeder et al. 2005)

$$\mathrm{SNR}_{\mathrm{ROI}} = \frac{S_{\mathrm{ROI}}}{\sigma_{\mathrm{ROI}}} = \frac{\mathrm{mean}(\mathbf{S}_1 + \mathbf{S}_2)|_{\mathrm{ROI}}}{\sqrt{2}\,\mathrm{std}(\mathbf{S}_1 - \mathbf{S}_2)|_{\mathrm{ROI}}}, \tag{9}$$

where the signal in the original image, S_{ROI} is half the average signal from the ROI in the sum image $(\mathbf{S}_1 + \mathbf{S}_2)$, i.e., $S_{\mathrm{ROI}} = \mathrm{mean}(\mathbf{S}_1 + \mathbf{S}_2)|_{\mathrm{ROI}}/2$, and the standard deviation of the noise in the original image is the standard deviation in the ROI of the difference image $(\mathbf{S}_1 - \mathbf{S}_2)$ divided by $\sqrt{2}$, i.e., $\sigma_{\mathrm{ROI}} = \mathrm{std}(\mathbf{S}_1 - \mathbf{S}_2)|_{\mathrm{ROI}}/\sqrt{2}$. The additional factor of $\sqrt{2}$ arises from the fact that when two images are added or subtracted, the variance of the new signal equals the sum of the variance of the noise of the two images, and the variance is simply the square of the standard deviation. If variations in noise across the region of interest are small, an accurate measurement of the local SNR is possible.

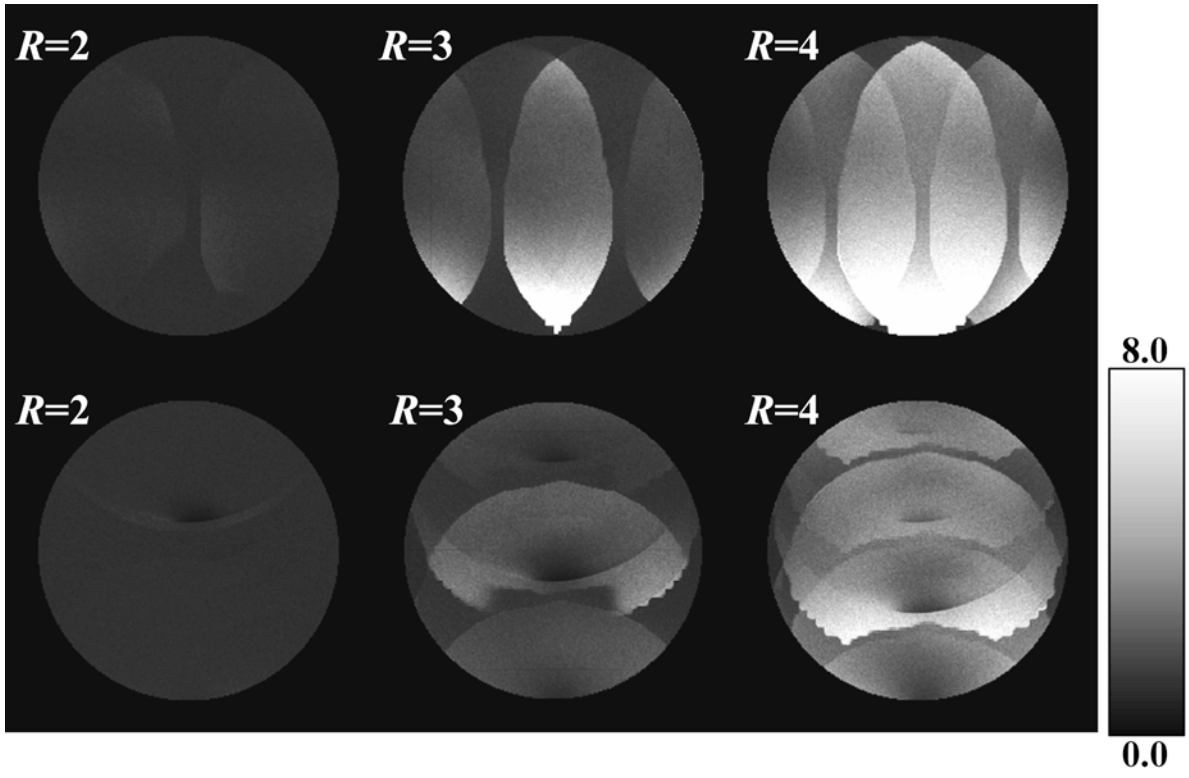

Fig. 4.8. Calculated g-factor images using Eq. (6) and the multiple acquisition method that acquired 200 consecutive spoiled gradient-echo images of a spherical phantom, such as those shown in Fig. 4.5. The phase-encoding direction is in the left–right direction (*top row*) and up–down direction (*bottom row*) for different acceleration factors (*R*).

This approach is known as the "difference method" and is shown schematically in Fig. 4.9.

The main advantage of the difference method is that only two images are required making in vivo measurements of SNR feasible. As with the multiple acquisition method, the signal must not fluctuate between the two images, or inaccurate SNR estimates will result. The main disadvantage of this method is that the effective spatial resolution of this method is lower and variations in SNR are "averaged" out over the ROI. For most clinical applications this is not a problem if small ROIs are used. In fact, this concept has been explored by Gizweski et al. (2005) by using a "sliding ROI" approach in conjunction with the difference method in order to generate a low-resolution SNR image.

The error on the estimates of the SNR in the region of interest is determined by the local SNR and the size of the ROI. It can be shown that the error on the estimate of SNR using the difference method is given by (Reeder et al. 2005)

$$\sigma_{SNR} \approx \mathrm{SNR}\sqrt{\frac{2}{N_{ROI}}}, \tag{10}$$

where N_{ROI} is the size of the ROI in pixels. For example, there will be an error of ±4 in the SNR measurement when the SNR is approximately 20 (i.e., a 20% error), when using an ROI of 50 pixels. Increasing the size of the ROI decreases this area but may average out variations in the local SNR.

Estimates of the g-factor can also be made with the difference method. This approach requires the acquisition of four images, two with an acceleration, R, and two with no acceleration. The difference of each pair of images can be used to estimate the standard deviation of the noise in the ROI of both accelerated and unaccelerated images. The g-factor is subsequently determined from Eq. (6), i.e.,

$$g = \frac{\mathrm{std}\left(S_1^R - S_2^R\right)}{\mathrm{std}\left(S_1^0 - S_2^0\right)\sqrt{R}}, \tag{11}$$

where $\mathrm{std}\left(S_1^R - S_2^R\right)$ is the standard deviation in the ROI of the difference of the accelerated images, and $\mathrm{std}\left(S_1^0 - S_2^0\right)$ is the standard deviation of the difference of the unaccelerated images. This approach has been shown to have very close agreement with the multiple acquisition method (Reeder et al. 2005). It

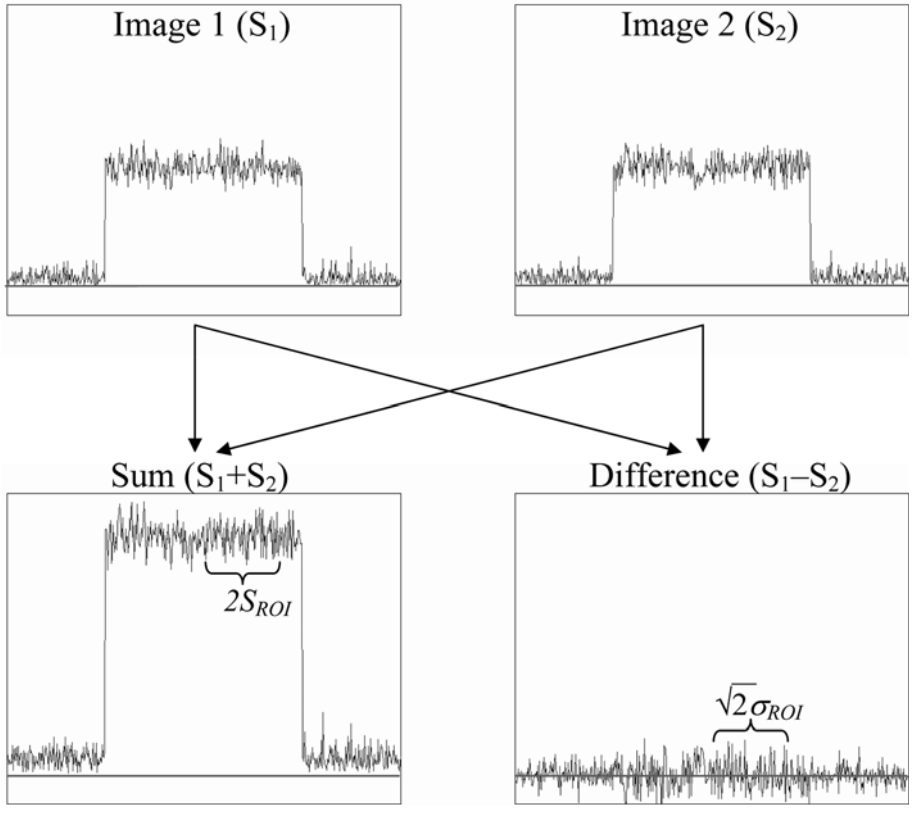

Fig. 4.9. The difference method. The average signal in the region of interest (ROI) of the sum image is twice the signal in the original images (S_{ROI}). The standard deviation in the ROI of the difference image equals $\sqrt{2}$ times the standard deviation of the noise in the original images (σ_{ROI}).

is important to use small ROIs with this approach, because an ROI that spans a sharp transition in the g-factor (e.g., Fig. 4.8) could lead to inaccurate estimation of the g-factor.

4.4.3 SNR Ratio Method

There are many situations where measurement of absolute SNR is not necessary, but the relative SNR may be sufficient. For example, flip-angle optimization may require acquisition of multiple images with identical imaging parameters except for the flip angle. The flip angle that generates the highest relative SNR or CNR in a particular tissue is then chosen.

For situations such as these where few parameters have changed, the SNR ratio method may be applicable; specifically, if parameters that affect the g-factor, such as field of view, matrix size, phase-encoding direction, coil sensitivities, the parallel-imaging acceleration factor or reconstruction algorithm, etc., *are unchanged between scans*. This means that the SNR ratio method cannot be used to analyze the SNR in comparisons of acquisitions with and without parallel imaging or with different acceleration factors as is often required in clinical studies.

To determine the SNR ratio, the average signal from one ROI in the area of interest (S_1, S_2), and the standard deviation of signal measured in a background "noise" ROI outside the body (σ_1, σ_2) are measured in both images, such that

$$\text{SNR Ratio} = \frac{\text{SNR}_1}{\text{SNR}_2} = \frac{S_1 \Big/ \left(\frac{g_{1,S}}{g_{1,\sigma}} \sigma_1 \right)}{S_2 \Big/ \left(\frac{g_{2,S}}{g_{2,\sigma}} \sigma_2 \right)} = \frac{S_1 \sigma_2}{S_2 \sigma_1} \qquad (12)$$

where $g_{i,S}$ is the g-factor at the ROI in the area of interest and $g_{i,\sigma}$ is the g-factor in the background "noise" ROI in images *i=1, 2*.

The SNR ratio method relies on the assumption that the g-factor is identical in the two images, i.e., $g_{1,S} = g_{2,S}$ and $g_{1,\sigma} = g_{2,\sigma}$. Accordingly, it is important to emphasize that the ROIs to determine signal and noise must be identical between the two images. In addition, the measurement of the signal and standard deviation cannot be used to measure the absolute SNR of that image for reasons discussed above. It is also noted that some reconstruction algorithms for parallel imaging set the background signal to 0. In this case the SNR ratio method cannot be applied since $\sigma_1 = \sigma_2 = 0$.

4.4.4 Direct Calculation of the g-Factor

As shown in the original description of the g-factor by Pruessmann et al. (1999), it is possible to calculate the g-factor directly if the coil sensitivities and noise correlation between separate coils is known. The coil sensitivities are complex (i.e., have magnitude and phase) which is information that is not typically available to most scanner operators. In addition, measurement of the noise correlation between the different coils requires additional measurements, and the calculation of g-factor images is complicated.

Recently, an elegant characterization of all noise contributions in an MR system has been performed by Kellman and McVeigh (2005) permitting the reconstruction of MR images with image intensity equal to SNR. In this work, noise contributions from coils, amplifiers, and filters, as well as additional noise amplification from parallel unwrapping, is calculated directly. Measurements of noise correlation between different coils are made during "pre-scan," and in combination with complex coil sensitivities, can be used to generate g-factor images directly. Examples of cardiac CINE images acquired with SSFP and TSENSE acceleration are shown in Fig. 4.10 along with their corresponding g-factor maps. Although this approach is more complicated and must be incorporated directly into the raw data reconstruction by the manufacturer of the imaging system, it provides robust and accurate estimates of SNR and the g-factor without additional image acquisition. The details of this work are beyond the scope of this chapter.

4.5 Special Considerations

4.5.1 TSENSE

The SNR performance of TSENSE (cf. Chap. 12) has the added benefit of temporal filtering. This SNR benefit is characterized by a simple modification of Eq. (4), specifically,

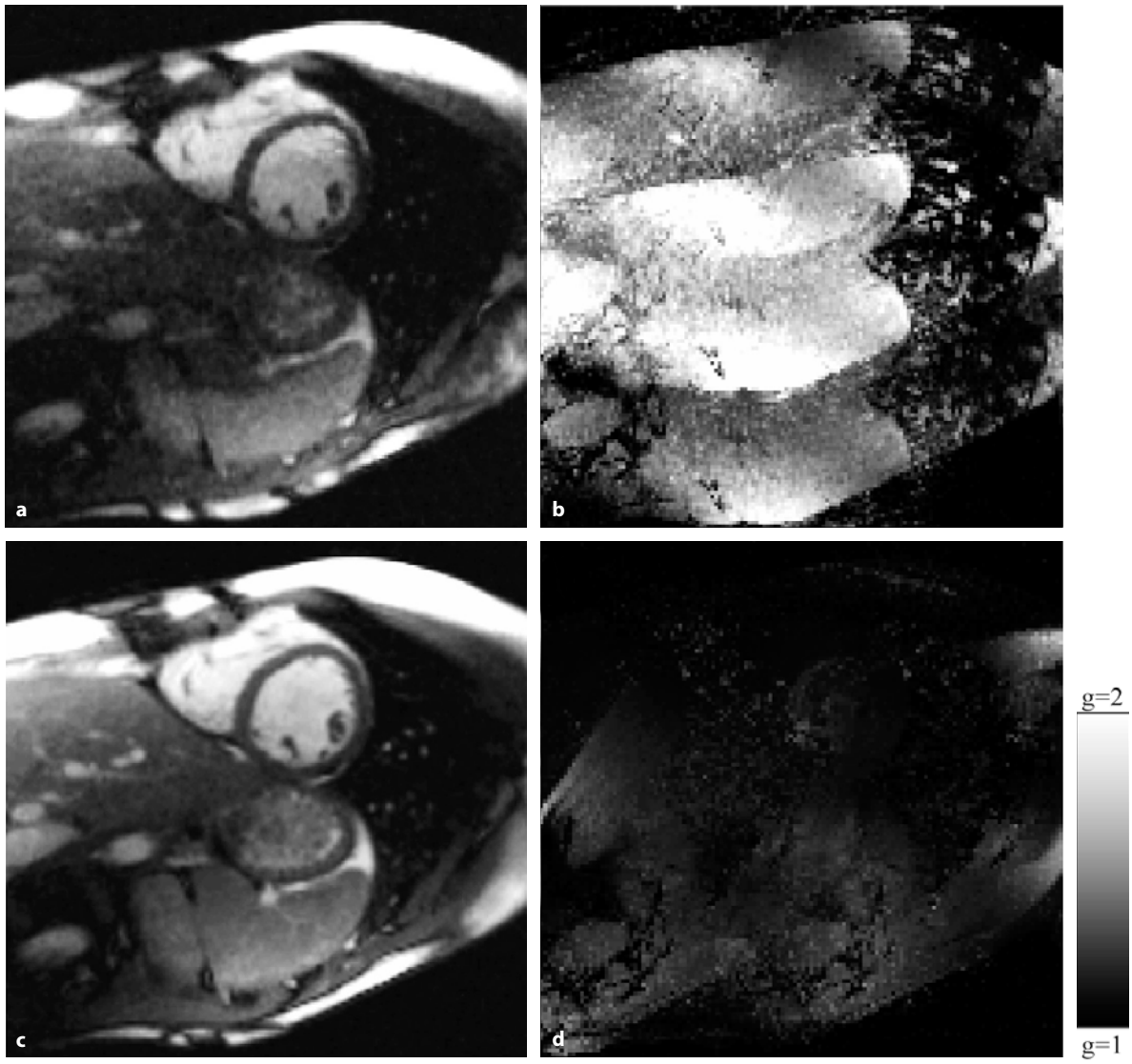

Fig. 4.10a–d. a,c Short-axis CINE SSFP images and **b,d** the corresponding g-factor images acquired using TSENSE (R=4) with the phase-encoding direction in the anterior–posterior direction (**a,b**) and in the left–right direction (**c,d**). The same scaling has been displayed for the g-factors. Note the strong dependence of the g-factor on phase-encoding orientation. (Courtesy of P. Kellman)

$$\mathrm{SNR} = \frac{\mathrm{SNR}_0}{g\sqrt{R}}\sqrt{\frac{\mathrm{BW}_{\mathrm{FULL}}}{\mathrm{BW}_{\mathrm{UNFOLD}}}}, \qquad (13)$$

where $\mathrm{BW}_{\mathrm{FULL}}$ and $\mathrm{BW}_{\mathrm{UNFOLD}}$ are the two-sided noise-equivalent temporal bandwidths for the full and reduced FOV acquisitions, respectively (Kellman et al. 2001). This filtering occurs in the time domain, by assuming relatively slow changes in the object between CINE image frames, allowing some temporal filtering to reduce image noise. Typically, $\mathrm{BW}_{\mathrm{FULL}}/\mathrm{BW}_{\mathrm{UNFOLD}} = 0.8$ improving SNR slightly. Knowledge of temporal filtering, if any, must be known before accurate estimates of the g-factor can be made using TSENSE.

4.5.2 Self-Calibrating Parallel-Acceleration Methods

As described in Chapter 2, parallel-imaging methods, such as generalized autocalibrating partial parallel acquisitions (GRAPPA), auto-SMASH (Jakob et al. 1998), and other variable density k-space sampling

methods (McKenzie et al. 2002), maintain full sampling at the center of k-space in order to obtain calibration information for unwrapping of undersampled outer regions of k-space. In many k-space-based reconstruction algorithms, these central calibration lines contribute to the reconstruction of the final image. This adds tremendous complexity to the SNR analysis of these images, because the central lines of k-space provide most of the contrast information in an image and carry most of the image *power* that primarily affects SNR. Higher spatial frequencies that carry important edge information are under-sampled and the noise distribution will be non-uniform across the image.

For these reasons, the measurement of SNR and g-factors should be applied very carefully to parallel imaging methods that use variable density k-space sampling. The multiple acquisition method remains valid because the noise distribution is still Gaussian in time. The difference method, however, will only be valid if the noise distribution is uniform across the ROI used. In general, this will not be true and caution should be exercised when using this method; however, *calculation of the g-factor may no longer be valid.* What is the effective acceleration factor that should be used in Eqs (4)–(6)? It is not simply the absolute time acceleration, because the undersampling of k-space is not uniform, and central k-space lines are weighted more heavily than higher spatial frequencies. Full characterization of SNR and the g-factor using variable-density k-space methods will prove very complex, and further work on this topic is required.

4.5.3 Measurement of SNR with Multi-Phase Contrast-Enhanced Imaging

Rapid, contrast-enhanced imaging, such as MR angiography or dynamic contrast-enhanced (DCE) imaging of solid organs (liver, brain, heart, etc.), are often combined with parallel-imaging applications in order to improve both temporal and spatial resolution of the acquisition. Measurement of SNR as well as contrast-to-noise ratio (CNR) between the background tissue and enhancing vessels/tissue is an important measure of the performance of these methods.

A variation in the difference method provides an opportunity to measure SNR in these circumstances. In this approach, at least two baseline non-contrast-enhanced images are required. As shown schematically in Fig. 4.11, estimates of the noise are made from the difference of two baseline images, $\mathbf{S}_1$ and $\mathbf{S}_2$. The local noise of $\mathbf{S}_1$ and $\mathbf{S}_2$ within an ROI is σ, which can be determined from the standard deviation of the difference image $(\mathbf{S}_1 - \mathbf{S}_2)$, i.e., . Signal enhancement is then determined from the difference of the enhanced image ($\mathbf{S}_3$) and a background image ($\mathbf{S}_1$ or $\mathbf{S}_2$), and is simply given by $\Delta S = \text{mean}(\mathbf{S}_3 - \mathbf{S}_2)|_{ROI}$; therefore,

$$\Delta\text{SNR} = \frac{\Delta S}{\sigma} = \frac{\sqrt{2}\,\text{mean}(\mathbf{S}_3 - \mathbf{S}_2)|_{\text{ROI}}}{\text{std}(\mathbf{S}_1 - \mathbf{S}_2)|_{\text{ROI}}}, \tag{14}$$

representing the SNR of the signal enhancement in the unsubstracted image, $\mathbf{S}_3$. More importantly, the SNR of the subtracted image $(\mathbf{S}_3 - \mathbf{S}_2)$, which is commonly used for visualization of angiographic images will have higher noise (by a factor of $\sqrt{2}$), such that

$$\Delta\text{SNR}_{\text{Diff}} = \frac{\Delta S}{\sigma} = \frac{\text{mean}(\mathbf{S}_3 - \mathbf{S}_2)|_{\text{ROI}}}{\text{std}(\mathbf{S}_1 - \mathbf{S}_2)|_{\text{ROI}}}. \tag{15}$$

Equations (14) and (15) provide a useful method of measuring the SNR of the signal enhancement that occurs with MRA or DCE imaging applications. It is valid with parallel imaging applications where the noise may be non-uniform across the image, and takes advantage of the multiple images acquired during the acquisition to determine noise and signal enhancement within the same ROI. It is important to note that these calculations must be performed with 2D planar images, and cannot be performed with maximum intensity projection (MIP) images that are commonly used to display angiographic images.

4.6 Summary and Conclusion

The measurement of SNR and CNR becomes increasingly important for parallel imaging applications where the overall amount of data is reduced, challenging the SNR performance of these techniques. Accurate evaluation of these methods is essential and an understanding of the limitations of conventional SNR measurement methods is crucial to avoid incorrect methods that can lead to erroneous estimates of SNR. The key concept is that from an SNR perspective, parallel imaging differs from conventional imaging by the fact that noise may have a non-uniform distribution across the image. Valid SNR measurement methods must determine both *the*

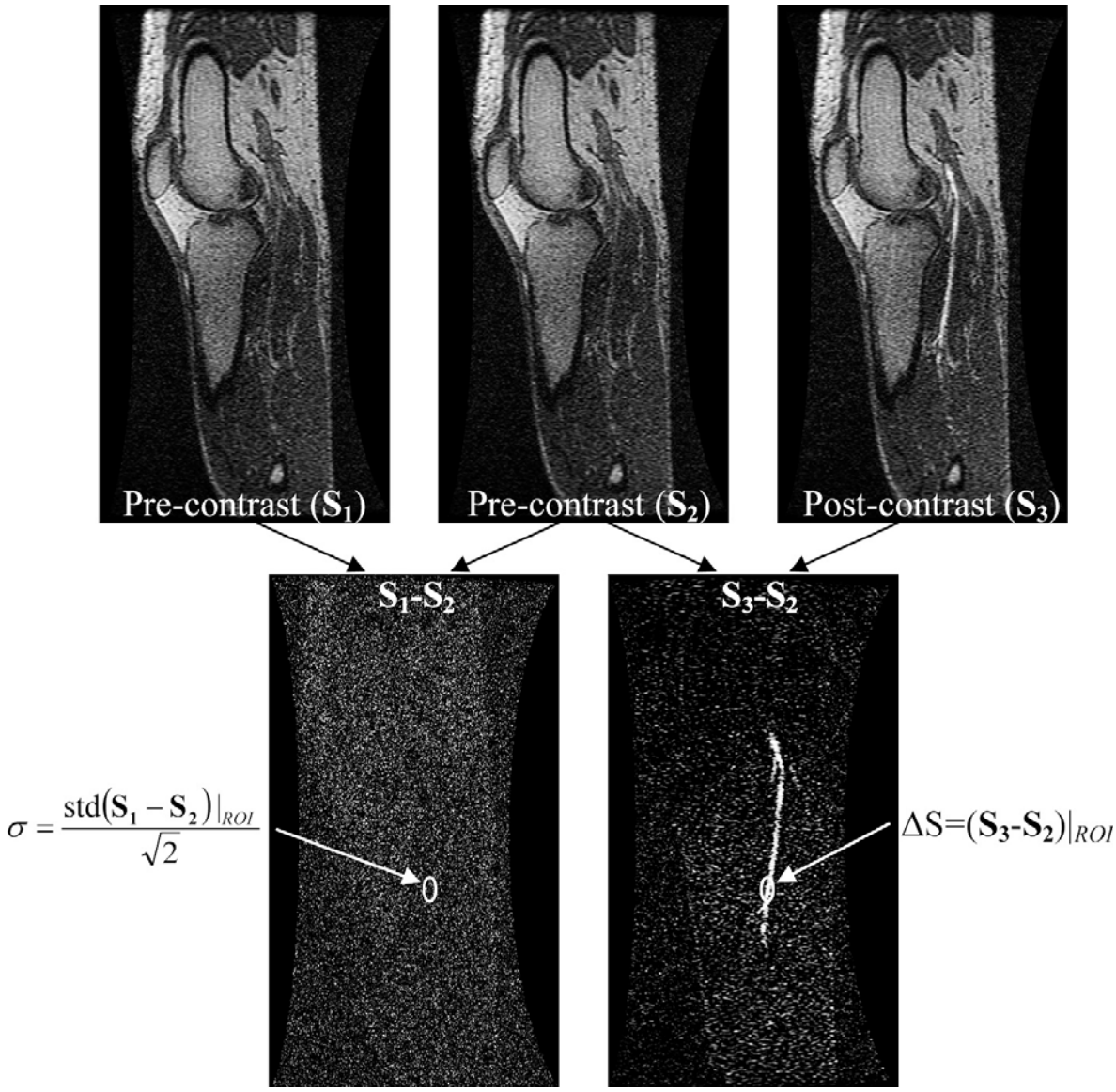

Fig. 4.11. The difference method applied to multi-phase contrast-enhanced angiography. The difference between two pre-contrast images is used to determine the noise, and the difference of the post-contrast and pre-contrast image is used to determine the signal enhancement, facilitating a quantitative SNR measurement of the contrast enhancement, even in the presence of non-uniform noise. Note that the ROI is larger than the vessel for illustrative purposes only, and should be chosen to "fit" the area of interest more accurately.

signal and noise within the same region of interest. In this chapter, we review the multiple acquisition and difference methods in detail in order to measure SNR and determine the g-factor. A variation in the difference method is described for measurement of SNR with dynamic contrast-enhanced and angiographic imaging. Finally, a new method that involves direct characterization of the system SNR permitting direct calculation of the g-factor is briefly discussed, although this approach may be complicated for most practitioners.

Acknowledgements. I thank A. Brau, PhD, for her assistance with the pulse sequence used to obtain the phantom images, as well as P. Kellman, PhD, and M. Griswold, PhD, for helpful discussions.

References

Bevington P, Robinson D (1992) Data reduction and error analysis for the physical sciences. McGraw-Hill, New York

Constantinides CD, Atalar E, McVeigh ER (1997) Signal-to-noise measurements in magnitude images from NMR phased arrays. Magn Reson Med 38:852–857

Edelstein W, Bottomley P, Pfeifer L (1984) A signal-to-noise calibration procedure for NMR imaging systems. Med Phys 11:180–185

Firbank MJ, Coulthard A, Harrison RM, Williams ED (1999) A comparison of two methods for measuring the signal to noise ratio on MR images. Phys Med Biol 44:N261–N264

Gizewski ER, Maderwald S, Wanke I, Goehde S, Forsting M, Ladd ME (2005) Comparison of volume, four- and eight-channel head coils using standard and parallel imaging. Eur Radiol 15:1555–1562

Griswold MA, Jakob PM, Nittka M, Goldfarb JW, Haase A (2000) Partially parallel imaging with localized sensitivities (PILS). Magn Reson Med 44:602–609

Griswold MA, Jakob PM, Heidemann RM et al. (2002) Generalized autocalibrating partially parallel acquisitions (GRAPPA). Magn Reson Med 47:1202–1210

Henkelman RM (1985) Measurement of signal intensities in the presence of noise in MR images. Med Phys 12:232–233

Jakob PM, Griswold MA, Edelman RR, Sodickson DK (1998) AUTO-SMASH: a self-calibrating technique for SMASH imaging. SiMultaneous Acquisition of Spatial Harmonics. Magma 7:42–54

Kellman P, McVeigh E (2005) Image reconstruction in SNR units, 2005. Proc Int Soc Mag Reson Med 13:2430

Kellman P, Epstein FH, McVeigh ER (2001) Adaptive sensitivity encoding incorporating temporal filtering (TSENSE). Magn Reson Med 45:846–852

McKenzie CA, Yeh EN, Ohliger MA, Price MD, Sodickson DK (2002) Self-calibrating parallel imaging with automatic coil sensitivity extraction. Magn Reson Med 47:529–538

McVeigh ER, Henkelman RM, Bronskill MJ (1985) Noise and filtration in magnetic resonance imaging. Med Phys 12:586–591

Price RR, Axel L, Morgan T et al. (1990) Quality assurance methods and phantoms for magnetic resonance imaging: report of AAPM Nuclear Magnetic Resonance Task Group No. 1. Med Phys17:287–295

Pruessmann KP, Weiger M, Scheidegger MB, Boesiger P (1999) SENSE: sensitivity encoding for fast MRI. Magn Reson Med 42:952–962

Reeder S, Wintersperger B, Dietrich O et al. (2005) Practical approaches to the evaluation of SNR performance with parallel imaging: application with cardiac imaging and a 32-channel cardiac coil. Magn Reson Med 54:748–754

Roemer PB, Edelstein WA, Hayes CE, Souza SP, Mueller OM (1990) The NMR phased array. Magn Reson Med 16:192–225

Sodickson DK, Manning WJ (1997) Simultaneous acquisition of spatial harmonics (SMASH): fast imaging with radiofrequency coil arrays. Magn Reson Med 38:591–603